MolecularMedicine

# Loss of Allograft Inflammatory Factor-1 Ameliorates Experimental Autoimmune Encephalomyelitis by Limiting Encephalitogenic CD4 T-Cell Expansion

*Prameladevi Chinnasamy,[1,2] Sarah E Lutz,[3*†] Dario F Riascos-Bernal,[1,2*] Venkatesh Jeganathan,[4] Isabel Casimiro,[1,2‡] Celia F Brosnan,[3] and Nicholas ES Sibinga[1,2,5]*

[1]Department of Medicine (Cardiovascular Division), [2]Department of Developmental and Molecular Biology, [3]Department of Neuroscience, and [5]Wilf Family Cardiovascular Research Institute, Albert Einstein College of Medicine, Bronx, New York, United States of America; and [4]Center for Autoimmune and Musculoskeletal Disease, The Feinstein Institute of Medical Research, Manhasset, New York, United States of America; [†]current affiliation: Department of Developmental & Cell Biology, University of California, Irvine, Irvine, California, United States of America; [‡]current affiliation: Department of Medicine, University of Chicago, Chicago, Illinois, United States of America

Experimental autoimmune encephalomyelitis (EAE), an animal model of human multiple sclerosis (MS), is mediated by myelin-specific autoreactive T cells that cause inflammation and demyelination in the central nervous system (CNS), with significant contributions from activated microglia and macrophages. The molecular bases for expansion and activation of these cells, plus trafficking to the CNS for peripheral cells, are not fully understood. Allograft inflammatory factor-1 (Aif-1) (also known as ionized $Ca^{2+}$ binding adapter-1 (Iba-1)) is induced in leukocytes in MS and EAE; here we provide the first assessment of Aif-1 function in this setting. After myelin oligodendrocyte glycoprotein peptide ($MOG_{35–55}$) immunization, Aif-1–deficient mice were less likely than controls to develop EAE and had less CNS leukocyte infiltration and demyelination; their spinal cords contained fewer CD4 T cells and microglia and more CD8 T cells. These mice also showed significantly less splenic CD4 T-cell expansion and activation, plus decreased proinflammatory cytokine expression. These findings identify Aif-1 as a potent molecule that promotes expansion and activation of CD4 T cells, plus elaboration of a proinflammatory cytokine milieu, in $MOG_{35–55}$-induced EAE and as a potential therapeutic target in MS.

**Online address: http://www.molmed.org**
**doi: 10.2119/molmed.2014.00264**

## INTRODUCTION

Multiple sclerosis (MS) is a chronic progressive disorder caused by the formation of inflammatory plaques in the brain and spinal cord (1). Experimental autoimmune encephalomyelitis (EAE) shares both neuropathological and clinical features of MS (2). Studies of MS and EAE provide evidence that T lymphocytes specific for myelin antigens contribute to disease pathogenesis (3). Inflammation in EAE is mediated by major histocompatibility complex (MHC) class II–restricted, Th1-type $CD4^+$ myelin reactive, and Th17-type T cells (4–6). Autoreactive T cells activate in the periphery, cross the blood-brain barrier to enter the central nervous system (CNS) and serve as important disease initiators, affecting both the local cytokine milieu and the recruitment and activation of various effector cells (7–9). Microglia and macrophages also contribute to EAE; they produce cytokines that promote inflammation during induction, but also phagocytose and clear apoptotic cell bodies, debris and inhibitory substances that limit remyelination and axon regeneration (10,11). The molecular mechanisms that control expansion, activation and CNS trafficking of myelin-specific autoreactive T cells and the complex functions of microglia and macrophages in EAE are incompletely understood.

Allograft inflammatory factor-1 (Aif-1) (also known as ionized $Ca^{2+}$ binding adapter-1 [Iba-1]) is a 17-kDa, interferon (IFN)-γ–inducible, EF hand motif protein encoded within the class III region of the MHC (human chromosome 6p21.3, mouse chromosome 17B1) in an area densely clustered with inflammatory re-

**SEL and DFR-B contributed equally to this work.*

***Address correspondence to*** *Nicholas ES Sibinga, Albert Einstein College of Medicine, Forchheimer G46, 1300 Morris Park Avenue, Bronx, NY 10461. Phone: 718-430-2881; Fax: 718-430-8989: E-mail: nicholas.sibinga@einstein.yu.edu.*

*Submitted December 30, 2014; Accepted for publication December 30, 2014; Published online (www.molmed.org) January 6, 2015.*

sponse genes (12,13). Largely similar gene products arising from the same locus have been named Iba1, microglial response factor-1 (MRF1) and daintain; Iba1 in particular is a well-known histologic marker of microglia and of their activation in pathological CNS conditions. Aif-1 is differentially expressed in various mouse and human tissues (14,15) and in multiple leukocyte types including macrophages and T cells at basal levels (16–18). In inflammatory disease models, upregulated Aif-1 expression has been reported in microglia, macrophages, T cells, synoviocytes, pancreatic β-cells and adipocytes under various pathological conditions representing encephalomyelitis, uveitis, neuritis, arteriopathies, arthritis and diabetes, respectively (19).

The significance of increased Aif-1 expression in neuroinflammatory diseases such as EAE (20,21) has not been characterized. Overexpression of Aif-1 in MOLT-4 T cells increases proliferation, migration and activation (17) and in macrophage cell lines enhances production of interleukin (IL)-6, IL-12 and IL-10 (22). On the other hand, impaired Aif-1 function decreases microglial phagocytosis (23). Extrapolation from these *in vitro* findings suggests that Aif-1 deficiency might ameliorate EAE by limiting T cell and macrophage inflammatory activity, but could also allow cellular debris to accumulate, secondarily exacerbating inflammation and neurotoxicity and impairing regenerative processes. We recently developed an Aif-1–deficient mouse line (24) that can be used to determine the net effect of loss of Aif-1 in disease models.

## MATERIALS AND METHODS

### Animals

Aif-1–deficient mice were generated through a homologous recombination gene targeting strategy (24). The targeted *aif-1* allele was backcrossed onto the C57BL/6 strain for eight generations, and the corresponding knockout (*aif-1*$^{-/-}$) and wild-type (*wt*) littermates were bred in-house as homozygous or heterozygote lines in the barrier facility at the Albert Einstein College of Medicine. All experiments involving live animals were performed in accordance with protocols approved by the Institutional Animal Care and Use Committee of the Albert Einstein College of Medicine and complied with the *Guide for the Care and Use of Laboratory Animals* (25).

### Induction of EAE and Evaluation of Clinical Disease

EAE was induced in mice as previously described (26). Briefly, 10- to 12-wk-old male mice were immunized subcutaneously in the lower dorsum with 300 μg myelin oligodendrocyte glycoprotein ($MOG_{35–55}$) peptide (MEVGWYRSPFSRVVHLYRNGK; Celtek Bioscience, Nashville, TN, USA) in a 200 μL emulsion of incomplete Freund adjuvant (IFA) containing 5 mg/mL *Mycobacterium tuberculosis* H37RA (Difco Laboratories, Detroit, MI, USA). Subsequent to immunization, the mice received intraperitoneal injections of pertussis toxin (500 ng; List Biological Laboratories, Campbell, CA, USA) on the first day of sensitization and again after 2 d. We considered the day after MOG immunization as d 1. The EAE disease activity was scored as follows: 0, no symptoms; 1, floppy tail; 2, hindlimb weakness; 3, hindlimb paralysis; 4, forelimb and hindlimb paralysis; and 5, death.

### Histologic and Immunofluorescence Analysis of Spinal Cords

For pathological analysis, EAE mice were anesthetized at the time points indicated and perfused with phosphate-buffered saline (PBS) via cardiac puncture. The spinal cord was flushed by hydrostatic pressure by using PBS. The lumbar spinal cord was postfixed overnight with 4% paraformaldehyde, and the tissues were paraffin embedded. To assess infiltration, coronal sections (6-μm thickness) were stained with hematoxylin and eosin (H&E) and examined by using an Axioskop II microscope with an MRc camera (Zeiss, Thornwood, NY, USA) in the Albert Einstein College of Medicine Analytical Imaging Facility. The extent of infiltration was represented as an infiltrated area, which was quantified by measuring the individual area covered by positive hematoxylin staining (representing single or clustered nuclei) in the submeningium of each spinal cord section by using Photoshop CS3, version 10 software (Adobe, San Jose, CA, USA); the average was normalized to total white matter area and expressed as a percentage.

To assess demyelination, paraffin-embedded spinal cord sections were deparaffinized and blocked with 10% donkey serum for 1 h at room temperature followed by antigen retrieval. The sections were incubated with anti-mouse myelin basic protein (MBP) (BioLegend, San Diego, CA, USA) overnight at 4°C and incubated with donkey anti-mouse Alexa 548 (Life Technologies [Thermo Fisher Scientific Inc., Waltham, MA, USA]) for 1 h at room temperature. The counterstained slides were mounted in aqueous mounting medium containing 4,6-diamidino-2-phenylindole (DAPI) dihydrochloride hydrate (Electron Microscopy Sciences, Hatfield, PA, USA) and examined by using an Olympus IX 81 microscope (Olympus America, Center Valley, PA, USA) with motorized stage and a Cooke Sensicam QE air-cooled charged-coupled device (CCD) camera in the Albert Einstein College of Medicine Analytical Imaging Facility. The extent of demyelination was quantified (Adobe Photoshop) by measuring the area of non–MBP-stained white matter, normalized to total white matter area, and expressed as a percentage.

### Isolation of Mononuclear Cells from the CNS

Spinal cords were perfused and flushed by hydrostatic pressure, and the recovered tissues were homogenized and digested with collagenase A (2 mg/mL; Roche Diagnostics, Indianapolis, IN, USA) in RPMI 1640 at 37°C for 15 min. The digested tissues were filtered through a 100-μm cell strainer to obtain a single cell suspension and centrifuged at

500*g* for 5 min. Cell pellets from two mice in each group were pooled, resuspended in 70% Percoll (Sigma-Aldrich, St. Louis, MO, USA), overlaid with 30% Percoll and centrifuged at 200*g* for 15 min. The cell monolayer at the 70–30% interphase was collected and stained with various antibodies for flow cytometry, as described below.

### Flow Cytometry Analysis

At d 16 after EAE induction, spleen and peripheral lymph node cells were isolated, depleted of erythrocytes, blocked for Fc receptors RII/III with antibodies specific for CD16/CD32 (BD Biosciences, San Jose, CA, USA) and stained for surface markers with the following antibodies: anti-CD3-APC, anti-CD4-FITC, anti-CD8-PerCP, anti-B220-Pacific blue, anti-CD69-PE, anti-CD25-APC, anti-Foxp3-PE, anti-Gr1-PerCP, F4/80-PE (all from BD Biosciences), anti-CD45-Pacific blue (BioLegend) and anti-CD11b-APC (eBiosciences, San Diego, CA, USA). The stained cells were analyzed by fluorescence-activated cell sorting (FACS) (LSRII, BD Biosciences), and the data were analyzed using FlowJo software (Tree Star, Ashland OR, USA).

### T-Cell Activation and Proliferation

To evaluate T-cell activation, splenocytes from naive 10-wk-old *wt* and *aif-1*$^{-/-}$ mice were isolated and enriched for CD4 T cells by using an EasySep positive selection kit (Stemcell Technologies, Vancouver, BC, Canada). CD4 T cells were seeded in a 12-well plate ($3.5 \times 10^6$/well) and stimulated with either dimethyl sulfoxide or phorbol myristic acid (10 ng/mL) and ionomycin (500 ng/mL) in the presence of a protein transport inhibitor (GolgiPlug™, BD Biosciences; 1 μg/mL/$10^6$ cells) for 5 h. Cells were harvested and subjected to intracellular staining with anti–IL-2-FITC (BD Biosciences) and analyzed by FACS (LSRII). Data were analyzed using FlowJo software. To assess T-cell proliferation, splenocytes were stimulated with either α-CD3 (200 ng/mL) or $MOG_{35–55}$ (20 μg/mL) for 72 h, and proliferation was measured by adding [$^3$H]thymidine (25 μCi/mL) for the last 24 h of the assay. Incorporated [$^3$H]thymidine was measured by using a β-counter and expressed as counts per minute.

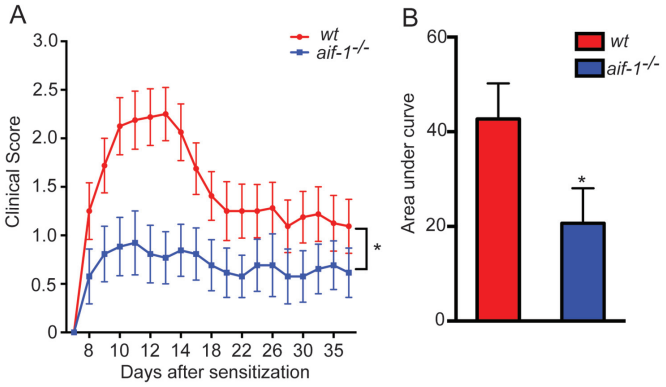


**Figure 1.** Aif-1 inactivation limits EAE in mice. *wt* and *aif-1*$^{-/-}$ mice were sensitized with $MOG_{35–55}$ and evaluated. (A) Clinical scoring of EAE activity in *wt* (n = 16) and *aif-1*$^{-/-}$ (n = 13) mice; data were pooled from two independent experiments and shown as mean ± SEM. (B) Clinical activity was quantified by measuring the area under the curve (AUC). The *P* values refer to comparison of *wt* and *aif-1*$^{-/-}$ mice. Data are represented as mean ± SEM. *$P < 0.05$.

### Cytokine Expression Analysis

Mononuclear cells were isolated from spleens of d-16 EAE-induced mice, and single cell suspensions were prepared in RPMI 1640 supplemented with 10% FBS, 1% penicillin-streptomycin, 1% L-glutamine and β-mercaptoethanol. Splenocytes ($4 \times 10^5$ cells/well) were stimulated with $MOG_{35–55}$ peptide (10 and 20 μg/mL) for 72 h. Cytokine levels in culture supernatants were determined by enzyme-linked immunosorbent assay (ELISA) by using antibodies to IL-6, IL-2, IFN-γ (BD Biosciences) and IL-12p40 (R&D Systems, Minneapolis, MN, USA).

### Real-Time Quantitative Polymerase Chain Reaction

Spleen tissues were homogenized with TRIzol (Life Technologies [Thermo Fisher Scientific]), and total RNA was extracted by using chloroform and precipitated with isopropanol. Synthesis of cDNA was performed by using 2 μg RNA using a reverse transcription system (Life Technologies [Thermo Fisher Scientific]). Real-time polymerase chain reaction was performed by using a Roche 480 light cycler using SYBR green quantitative master mix (Roche Applied Sciences, Indianapolis, IN, USA). The relative expression of cytokine and *iNOS* genes was determined in comparison to that of *gapdh*. Data were analyzed by using the Pfaffl method (27). The following primers were used: 5′-GCTAC CAAACTGGATATAATCAGGA-3′ and 5′-CCAGGTAGCTATGGTACTCCAGAA-3′ (*IL-6*); 5′-GATTCAGACTCCAGGGGACA-3′ and 5′-TGGTTAGCTTCTGAGGACAC ATC-3′ (*IL-12p40)*; 5′-CCATCAGCAG ATCATTCTAGACAA-3′ and 5′-CGCCA TTATGATTCAGAGACTG-3′ (*IL-12p35*); 5′-GCTGTTGATGGACCTACAGGA-3′ and 5′-TTCAATTCTGTGGCCTGCTT-3′ (*IL-2)*; 5′-CATCGGCATTTTGAACGAG-3′ and 5′-CGAGCTCACTCTCTGTGGTG-3′ (*IL-4*); 5′-ATCTGGAGGAACTGGCAAAA-3′ and 5′-TTCAAGACTTCAAAGAGTCT GAGGTA-3′ (*IFN-γ*); 5′-TCTTCTCATT CCTGCTTGTGG-3′ and 5′-GGTCT GGGCCATAGAACTGA-3′ (*TNF-α*); 5′-CAGGGAGAGCTTCATCTGTGT-3′ and 5′-GCTGAGCTTTGAGGGATGAT-3′ (*IL-17*); 5′-TCCCTACTAGGACTCAGCCA AC-3′ and 5′-TGGGCATCTGTTGGGTCT-3′ (*IL-23p19*); 5′-GGGCTGTCACGGAGA TCA-3′ and 5′-CCATGATGGTCACAT TCTGC-3′ (*iNOS*); 5′-CAGAGCCACA TGCTCCTAGA-3′ and 5′-GTCCAGCTGG TCCTTTGTTT-3′ (IL-10); 5′-CCTCTGACCC TTAAGGAGCTTAT-3′ and 5′-CGTTG CACAGGGGAGTCT-3′ (*IL-13*).

**Table 1.** Development of EAE in *wt* and *aif-1*$^{-/-}$ mice.

| Genotype | Day of onset[a] | Days to peak clinical disease[b] | Mean clinical score | Cumulative disease index (%)[c] | Incidence (%)[d] | Maximum score | Mortality |
|---|---|---|---|---|---|---|---|
| *wt* | 8.1 ± 0.61 | 10.1 ± 0.84 | 1.46 ± 0.13 | 28 ± 4.5 | 15/16 (94%) | 2.6 ± 0.26 | None |
| *aif-1*$^{-/-}$ | 8.6 ± 1.3 | 10.6 ± 0.84 | 0.67 ± 0.05*** | 13 ± 4.5* | 8/13 (62%) | 1.5 ± 0.33* | None |

Data are represented as mean ± SEM. *$P < 0.05$, ***$P < 0.0001$.
[a]Second consecutive day in which an animal scored ≥0.5.
[b]Time for each mouse to reach its highest score.
[c]Sum of the daily EAE scores for each mouse for entire duration of the experiment.
[d]Fraction of animals with scores ≥0.5 at a given time during the entire disease course.

### Statistical Analysis

Data are represented as mean ± standard error of the mean (SEM). Two-tailed Student *t* test, two-way analysis of variance and Mann-Whitney *U* test were used to assess statistical significance. *P* values <0.05 were considered statistically significant. Quantitative analyses were performed with Prism for Mac OSX (GraphPad Software).

*All supplementary materials are available online at www.molmed.org.*

## RESULTS

### Mice Lacking Aif-1 Show Lower Incidence and Reduced Clinical Severity of EAE

Aif-1 expression is induced in microglial cells in different stages of EAE in rat and mouse models (20,21), but its functional significance to EAE pathogenesis has not been previously tested. To determine how Aif-1 affects EAE disease activity, we immunized *wt* and *aif-1*$^{-/-}$ littermate controls with $MOG_{35–55}$ by using a standard protocol, as described in Materials and Methods. Compared to *wt* controls, *aif-1*$^{-/-}$ mice sensitized with $MOG_{35–55}$ developed less severe EAE (Figure 1A), as reflected in both mean clinical scores and overall clinical expression of disease (area under the curve [AUC], Figure 1B) throughout the disease evaluation period. Although the timing of disease onset and time to peak disease were similar in both groups (Table 1), *aif-1*$^{-/-}$ mice had reduced EAE incidence, maximum clinical score and cumulative disease index.

### Aif-1 Deficiency in Mice Decreases EAE-Associated CNS Leukocyte Infiltration and Demyelination

EAE is initiated by leukocyte infiltration in the CNS, which leads in turn to demyelination and axonal damage (28). To determine if neurological sparing in *aif-1*$^{-/-}$ mice was due to differences in leukocyte infiltration, we performed H&E staining of spinal cord sections from d-16 EAE-induced mice and found reduced inflammatory cell infiltrates in *aif-1*$^{-/-}$ compared with *wt* mice (Figures 2A, B). We stained sections for MBP and observed that myelination was relatively preserved in *aif-1*$^{-/-}$ mice (Figures 2C, D). Overall, these findings show that immune cell infiltration and demyelination were both significantly decreased in *aif-1*$^{-/-}$ spinal cords, consis-

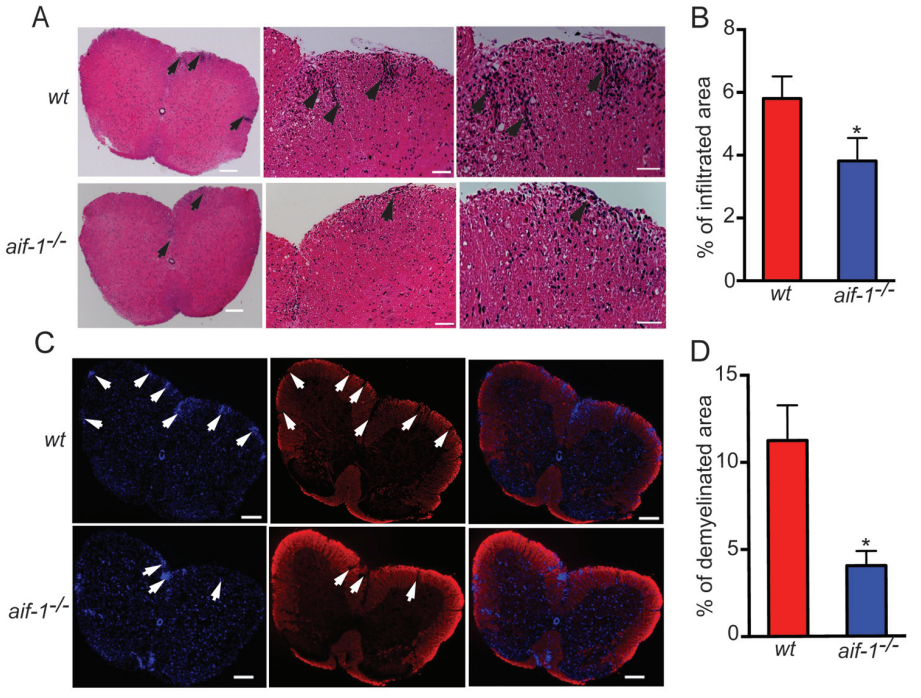


**Figure 2.** Loss of Aif-1 reduces $MOG_{35–55}$–induced CNS infiltration and demyelination. (A) H&E staining of d-16 EAE lesions from *wt* and *aif-1*$^{-/-}$ mice shows mononuclear cell infiltration in the submeningeal areas of lumbar spinal cord (indicated by arrows, scale bars: left panel, 200 μm; right panel, 20 μm). (B) Total infiltrates were quantified as described in Materials and Methods (n = 4). (C) MBP (red) with DAPI nuclear (blue) stains to assess demyelination; scale bars: 150 μm. (D) Demyelination was quantified in both groups (n = 4), as described in Materials and Methods. Data are represented as mean ± SEM. *$P < 0.05$.

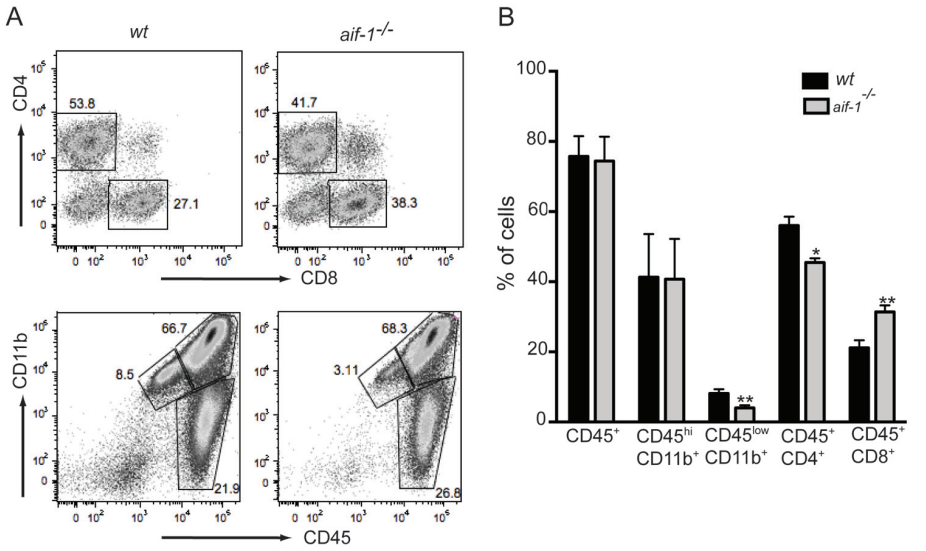


**Figure 3.** CNS immune cell infiltration is reduced in d-16 EAE *aif-1*$^{-/-}$ mice. (A) Representative FACS data (A) and quantification of effector T cells (B) (CD45$^{+}$ CD3$^{+}$CD4$^{+}$; CD45$^{+}$ CD3$^{+}$ CD8$^{+}$), microglia (CD45$^{low}$CD11b$^{+}$) and infiltrated monocytes/activated microglia (CD45$^{high}$CD11b$^{+}$) from spinal cords of *wt* and *aif-1*$^{-/-}$ mice (n = 6). Data are represented as mean ± SEM. *$P$ < 0.05, **$P$ < 0.01.

myelination in EAE, resulting in decreased disease incidence and severity.

### Aif-1 Promotes Expansion and Activation of Encephalitogenic CD4 T Cells in Spleen

In EAE, myelin-specific T cells are activated in the periphery and migrate into the CNS by crossing the blood-brain barrier (30,31). To investigate if the decreases in disease activity and CNS infiltration and preserved myelin observed in Aif-1–deficient mice (Figures 1–3) reflected differences in the immune response in the periphery, we analyzed leukocyte subsets in the spleens of d-16 EAE mice. FACS analyses of splenocytes from *wt* and *aif-1*$^{-/-}$ mice showed similar proportions of B cells and monocytes and no significant difference in the frequency or absolute number of CD3 T cells, but there was a reduced percentage of CD4 T cells with Aif-1 deficient with the decreased incidence and severity of disease.

### Aif-1 Deficiency Reduces CNS Infiltration by CD4 T Cells

We further evaluated the effect of Aif-1 deficiency on CNS leukocyte populations by profiling spinal cord mononuclear cells from d-16 EAE in *wt* and *aif-1*$^{-/-}$ mice by using FACS. Compared to *wt*, *aif-1*$^{-/-}$ spinal cords had fewer CD45$^{low}$CD11b$^{+}$ microglia, fewer CD4 T cells and more CD8 T cells. However, we found no difference in CD45$^{int\text{-}high}$ CD11b$^{+}$ activated microglia or infiltrated monocytes (Figures 3A, B). This decrease in microglia could reflect an essential role for Aif-1 in microglial survival or repopulation (29) at baseline. We addressed these possibilities by analyzing resident microglial populations (CD45$^{low}$CD11b$^{+}$) in *wt* and *aif-1*$^{-/-}$ naive mice by FACS and found no difference between the two groups (Supplementary Figure S1), which suggests that Aif-1 is not necessary for microglial survival or repopulation at baseline. Overall, our data show that Aif-1 inactivation limits its CNS CD4 T-cell infiltration and de-

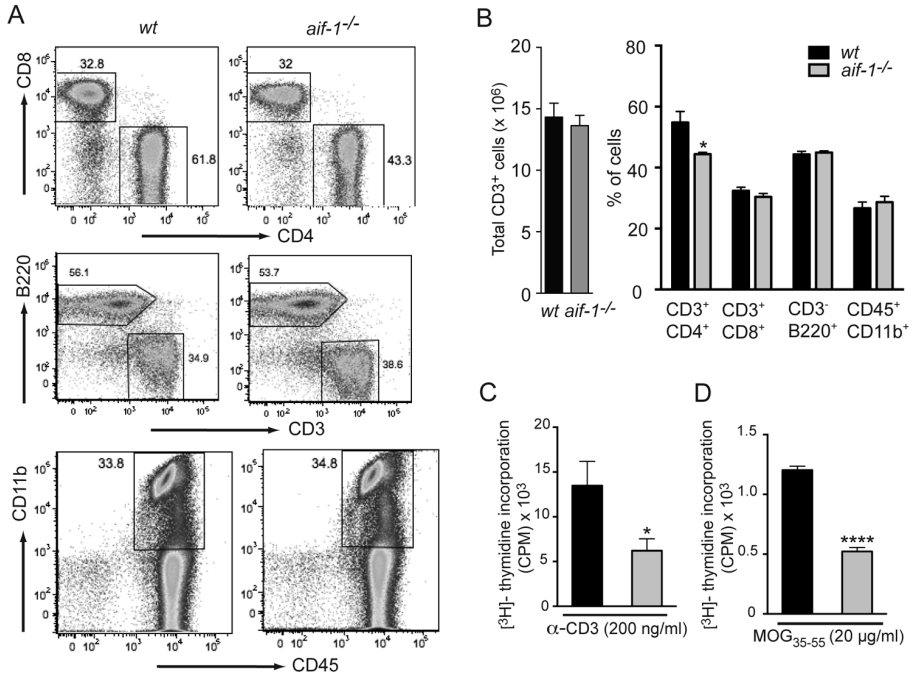


**Figure 4.** Aif-1 deficiency reduces CD4 T-cell expansion in the spleen. (A) Representative FACS data of effector T cells (CD3$^{+}$CD4$^{+}$; CD3$^{+}$CD8$^{+}$), B cells (CD3$^{-}$B220$^{+}$) and monocytes (CD45$^{+}$CD11b$^{+}$) from splenocytes of d-16 EAE *wt* and *aif-1*$^{-/-}$ mice. (B) Absolute quantification of CD3$^{+}$ splenocytes (left panel) and relative quantification of T-cell subsets, B cells and monocytes (right panel). (C, D) T-cell proliferation was measured by rechallenging splenocytes with α-CD3 antibodies and (D) $MOG_{35-55}$ to measure proliferation by ($^{3}$H)thymidine incorporation (n = 6). Data are represented as mean ± SEM. *$P$ < 0.05; ****$P$ < 0.0001.

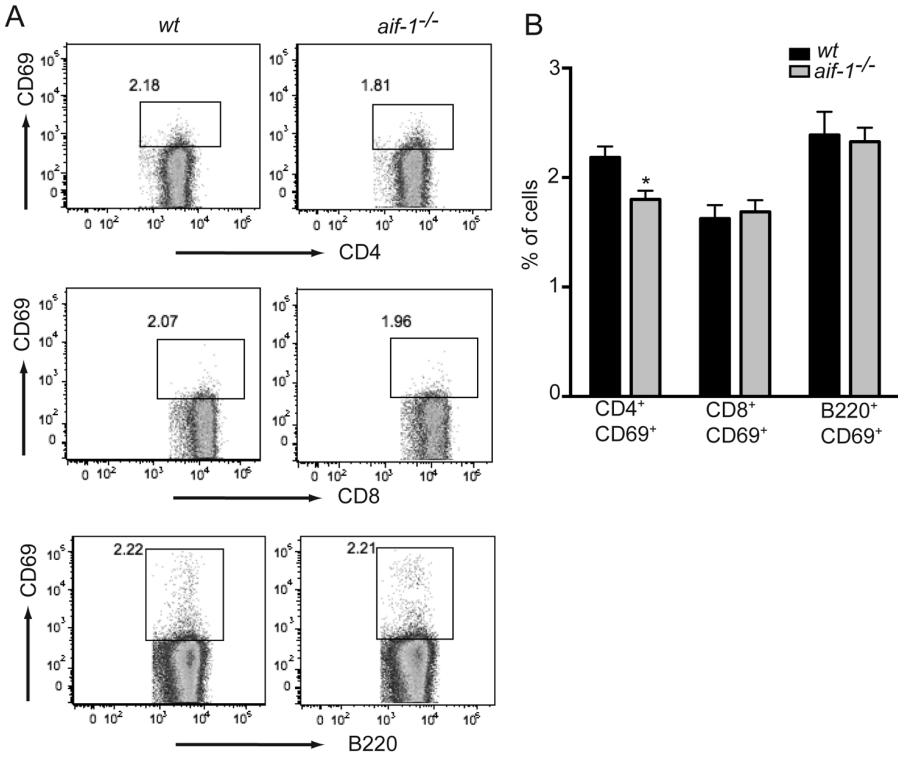


**Figure 5.** Aif-1 deficiency reduces CD4 T-cell activation in the spleen. (A) Representative FACS data and (B) quantification of activated CD4 T ($CD4^+CD69^+$), CD8 T ($CD8^+CD69^+$) and B ($B220^+CD69^+$) cells in spleens from *wt* and *aif-1*$^{-/-}$ mice at d-16 EAE (n = 6). Data are represented as mean ± SEM. *$P < 0.05$.

ciency (Figures 4A, B). We asked further whether the lower percentage of CD4 T cells observed in $MOG_{35–55}$ immunized Aif-1–deficient mice might reflect a developmental deficiency in T-cell subsets. In various immune cell populations from naive *wt* and *aif-1*$^{-/-}$ mice (splenocytes; Supplementary Figure S2A) and peripheral blood (not shown), and thymic T cells (Supplementary Figure S2B), FACS analysis failed to find significant genotype-dependent differences in T-cell subsets. These findings suggest that lack of Aif-1 does not affect baseline T-cell development, but limits the ability of CD4 T cells to expand in response to specific immunization.

To test this idea directly, we challenged splenocytes from previously immunized *wt* and *aif-1*$^{-/-}$ mice with either anti-CD3 or $MOG_{35–55}$. With both anti-CD3, as a general T-cell activator, or $MOG_{35–55}$ as a specific antigen rechallenge, cells from *aif-1*$^{-/-}$ mice proliferated less than *wt* control (Figures 4C, D). On the other hand, activation of T cells from naive *wt* and *aif-1*$^{-/-}$ mice by phorbol ester and ionomycin was equivalent (Supplementary Figure S3), which shows that the Aif-1 deficiency affects acquired but not basal T-cell responsiveness. Collectively, these data suggest that Aif-1 promotes myelin-specific CD4 T-cell expansion in the spleen, which in turn supports CD4 T-cell infiltration and demyelination of the spinal cord in EAE. Because antigen stimulation also promotes immune cell recruitment to and activation in lymph nodes, we further determined the effect of Aif-1 deficiency on lymph node populations after $MOG_{35–55}$ immunization; these studies showed no significant differences between *wt* and *aif-1*$^{-/-}$ mice in lymph node populations including T-cell subsets, B cells and monocytes (Supplementary Figure S4).

### Aif-1 Deficiency Promotes Th1 to Th2 Bias in Spleen

Autoreactive CD4 T cells and their associated proinflammatory cytokine milieu play important roles in the pathogenesis of EAE and MS. We assessed how lack of Aif-1 affected B and T lymphocyte activation and cytokine production in d-16 EAE splenocytes and found a modest decrease in CD4 T-cell activation ($CD4^+CD69^+$) in *aif-1*$^{-/-}$ mice relative to controls, but no differences in activation of CD8 T and B cells (Figures 5A, B). More importantly, compared with controls, EAE-induced *aif-1*$^{-/-}$ mice showed significantly reduced expression of IL-6, IL-2, IL-12p35, IL-12p40 and IFN-γ mRNA, but increased levels of IL-4 mRNA (Figure 6A), suggesting that Aif-1 deletion promotes a Th1 to Th2 switch in the spleen. Trends toward decreased tumor necrosis factor (TNF)-α, IL-13 and increased IL-10 levels were observed in *aif-1*$^{-/-}$ samples. We found no difference between the two groups in expression of other Th1 mRNA transcripts including inducible NO synthase (*iNOS*), *IL-17* and *IL-23* (Figure 6B). Consistent with these mRNA findings, antigen recall experiments showed significantly reduced levels of IL-6, IL-12p40, IL-2 and IFN-γ protein in supernatants of $MOG_{35–55}$-stimulated splenocytes from *aif-1*$^{-/-}$ mice compared with *wt* mice (Figure 6C), with no differences in the levels of TNF-α or IL-23 (not shown). Because we did not find differences in expression of either IL-23 or IL-17 between *wt* and *aif-1*$^{-/-}$ samples, we asked if the Th1 to Th2 switch with loss of Aif-1 could be due to an increase in induced regulatory T (iTreg) cells (32). We assessed iTreg populations in splenocytes and lymph node cells (Supplementary Figures S5A–D) from d-16 EAE mice by FACS and found no significant difference between the groups. Taken together, our data demonstrate that Aif-1 deficiency limits CD4 T-cell activation and the proinflammatory nature of the cytokine milieu in $MOG_{35–55}$-sensitized spleens, without affecting iTreg levels.

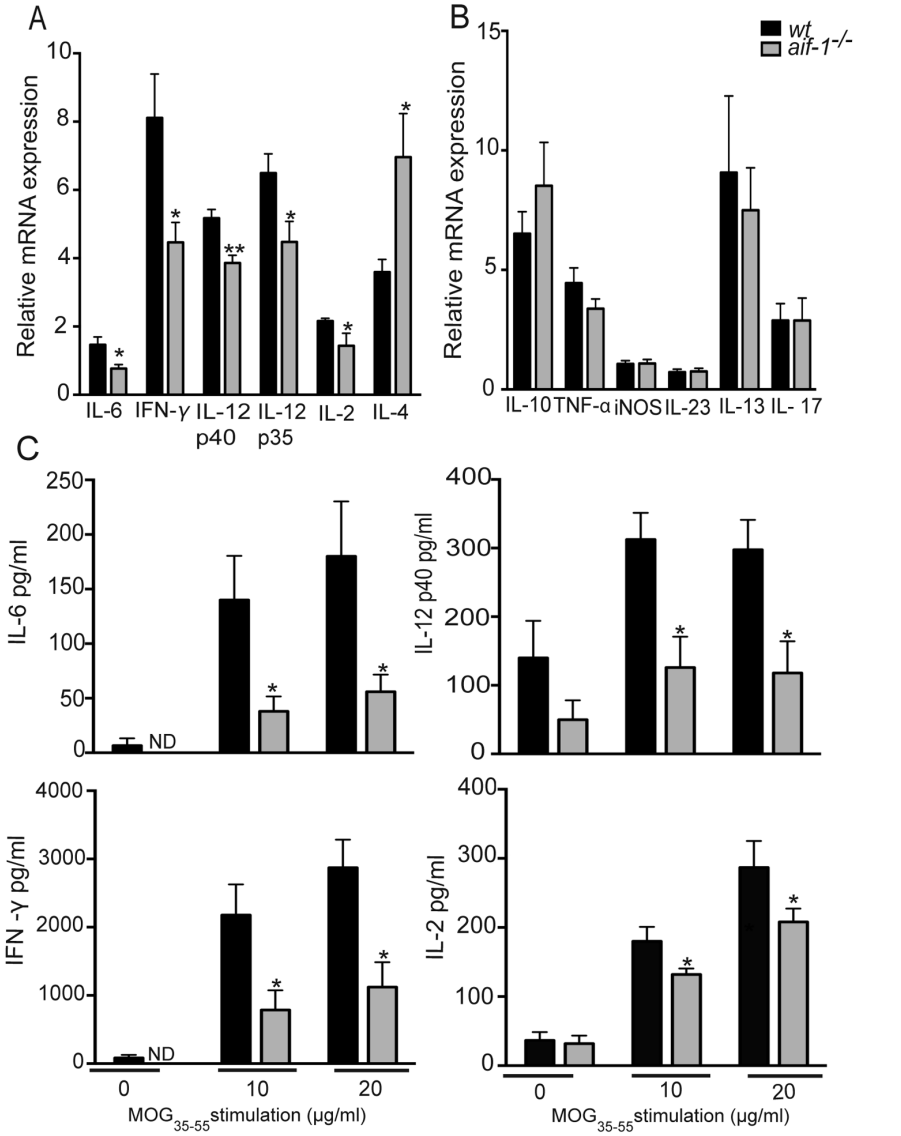


**Figure 6.** Aif-1 inactivation promotes a Th1 to Th2 switch in the periphery. (A, B) Relative cytokine mRNA expression measured in spleens from d-16 EAE *wt* and *aif-1*$^{-/-}$ mice, normalized to *gapdh* (n = 7). (C) Th1 cytokine expression after rechallenge with $MOG_{35–55}$, as measured by ELISA (n = 4). Data are represented as mean ± SEM. **P* < 0.05, ***P* < 0.01.

## DISCUSSION

Studies of both MS and EAE implicate myelin-specific T cells, macrophages and microglia as mediators of disease activity (3). Expression of Aif-1 increases above basal levels in these cell types (16–18) in neuro-inflammatory disease models (19). Conceivably, increased expression of Aif-1 during EAE pathogenesis (20,21) could promote T cell, macrophage and/or microglial proinflammatory functions and overall disease activity. Alternatively, Aif-1–dependent microglial phagocytosis (23) and clearance of cellular debris could be important as means to limit inflammation and enhance regenerative processes (11). We recently developed an Aif-1–deficient mouse model (24) that can be used to gain insight into the significance of Aif-1 expression in disease models. These mice do not show growth or fertility defects, or evidence of immunodeficiency in normal barrier housing conditions. To assess the relative importance of these different Aif-1 functions in the EAE model *in vivo*, we immunized *wt* and *aif-1*$^{-/-}$ littermate mice with $MOG_{35–55}$ peptide and characterized their clinical and pathological response.

Although baseline peripheral, splenic, thymic lymphocyte and CNS microglial populations were similar in *wt* and *aif-1*$^{-/-}$ mice, the Aif-1–deficient mice had lower incidence and severity of induced disease. This result corresponded to reduced CNS leukocyte infiltration and demyelination and was associated with impaired expansion and activation of myelin-specific CD4 T cells and decreased proinflammatory cytokine production in the periphery. These findings suggest that Aif-1–dependent proinflammatory activities are dominant in this setting, whereas its phagocytotic and clearance functions are less critical.

Interestingly, the effect of Aif-1 deficiency on leukocyte populations after immunization was relatively modest, with a decrease of ~10% in the number of both $CD3^+CD4^+$ and $CD4^+CD69^+$ T cells; on the other hand, proliferation of splenocytes lacking Aif-1 in response to either general anti-CD3 or specific $MOG_{35–55}$ antigen challenge was reduced by ~50%. This markedly impaired proliferative response was accompanied by a substantial reduction in several important Th1 cytokines, including IL-6, IFN-γ, IL-12 and IL-2, plus an increase in the Th2 cytokine IL-4, suggesting that loss of Aif-1 limits Th1-type immune responses while enhancing Th2-type immune responses. We found no differences in the iTreg cell population or in expression of markers of Th17 differentiation, including IL-23 p19 and IL-17. Nevertheless, because IL-12 p40 combines with IL-23 p19 to form functional IL-23 heterodimers, reduction of the former could limit IL-23 activity, which has been shown to be critical for EAE (33), particularly during disease induction (34).

The mechanistic basis for Aif-1–dependent effects on cytokine expression is not yet clear. Aif-1 localizes primarily to

the cytoplasm, and molecular functions ascribed to Aif-1 to date include actin bundling activity (35); it has also been linked to signaling via the small GTPase Rac (36,37), which itself is well known to affect actin cytoskeletal dynamics (38). The Aif-1 protein structure is notable for a conserved EF hand motif, although there are conflicting reports as to whether this is capable of binding $Ca^{2+}$ (39,40). Broad manipulations of the actin cytoskeleton, as with cytochalasin D or latrunculin B treatment, have been shown to affect relevant gene expression, including activity of the IL-2 gene promoter and $Ca^{2+}$-activated NFAT (nuclear factor of activated T-cells) transcription factors (41,42). It is possible that effects on actin cytoskeletal remodeling, Rac activation and/or $Ca^{2+}$ handling due to loss of Aif-1 impinge negatively on signaling pathways that support T-cell inflammatory gene expression. Alternatively, a recent study shows proinflammatory activity of recombinant Aif-1 added to monocytes (43). Although Aif-1 lacks a classical secretory motif, this observation suggests that it could have important effects as a released extracellular factor.

## CONCLUSION

These findings identify Aif-1 as a molecule that promotes Th1-helper CD4 T-cell expansion, activation and a proinflammatory cytokine milieu in $MOG_{35–55}$-induced EAE. Future studies with selective inactivation of Aif-1 will be required to assess the relative importance of Aif-1 in monocyte/macrophage and T lymphocyte lineages and to define the molecular mechanisms by which Aif-1 promotes autoreactive CD4 T-cell expansion, activation and inflammatory cytokine expression. Regardless of the specific mechanism at play, our results to date implicate Aif-1 as a potential target for MS therapy and provide support for the idea that inhibitors of Aif-1 expression or function may have beneficial effects on MS disease activity.

## ACKNOWLEDGMENTS

We thank the staff of the Albert Einstein College of Medicine Analytical Imaging Facility, FACS and Histology core facilities of Albert Einstein College of Medicine for their expert assistance. This work was supported in part by Pilot Project PP1500 from the National Multiple Sclerosis Foundation and by grant HL67944 from the National Institutes of Health.

## DISCLOSURE

The authors declare that they have no competing interests as defined by *Molecular Medicine*, or other interests that might be perceived to influence the results and discussion reported in this paper.

## REFERENCES

1. Frohman EM, Racke MK, Raine CS. (2006) Multiple sclerosis: the plaque and its pathogenesis. *N. Engl. J. Med.* 354:942–55.
2. Martin R, McFarland HF. (1995) Multiple sclerosis: are HLA class I molecules involved in disease pathogenesis? *Ann. Neurol.* 38:137–9.
3. Compston A, Coles A. (2008) Multiple sclerosis. *Lancet.* 372:1502–17.
4. Wekerle H, Kojima K, Lannes-Vieira J, Lassmann H, Linington C. (1994) Animal models. *Ann. Neurol.* 36 (Suppl.):S47–53.
5. Miller SD, Karpus WJ. (1994) The immunopathogenesis and regulation of T-cell-mediated demyelinating diseases. *Immunol. Today.* 15:356–61.
6. Langrish CL, *et al.* (2005) IL-23 drives a pathogenic T cell population that induces autoimmune inflammation. *J. Exp. Med.* 201:233–40.
7. Zhang R, *et al.* (2011) Amelioration of experimental autoimmune encephalomyelitis by beta-elemene treatment is associated with Th17 and Treg cell balance. *J. Mol. Neurosci.* 44:31–40.
8. Steinman L, Zamvil SS. (2005) Virtues and pitfalls of EAE for the development of therapies for multiple sclerosis. *Trends Immunol.* 26:565–71.
9. Domingues HS, Mues M, Lassmann H, Wekerle H, Krishnamoorthy G. (2010) Functional and pathogenic differences of Th1 and Th17 cells in experimental autoimmune encephalomyelitis. *PLoS One.* 5:e15531.
10. Napoli I, Neumann H. (2010) Protective effects of microglia in multiple sclerosis. *Exp. Neurol.* 225:24–8.
11. Jiang Z, Jiang JX, Zhang GX. (2014) Macrophages: a double-edged sword in experimental autoimmune encephalomyelitis. *Immunol. Lett.* 160:17–22.
12. Iris FJ, *et al.* (1993) Dense Alu clustering and a potential new member of the NF kappa B family within a 90 kilobase HLA class III segment. *Nat. Genet.* 3:137–45.
13. Deininger MH, Meyermann R, Schluesener HJ. (2002) The allograft inflammatory factor-1 family of proteins. *FEBS Lett.* 514:115–21.
14. Autieri MV, Haines DS, Romanic AM, Ohlstein EH. (1996) Expression of 14-3-3 gamma in injured arteries and growth factor- and cytokine-stimulated human vascular smooth muscle cells. *Cell Growth Differ.* 7:1453–60.
15. Hara H, *et al.* (1999) Isolation of two novel alternative splicing variants of allograft inflammatory factor-1. *Biol. Chem.* 380:1333–6.
16. Del Galdo F, Jimenez SA. (2007) T cells expressing allograft inflammatory factor 1 display increased chemotaxis and induce a profibrotic phenotype in normal fibroblasts in vitro. *Arthritis Rheum.* 56:3478–88.
17. Kelemen SE, Autieri MV. (2005) Expression of allograft inflammatory factor-1 in T lymphocytes: a role in T-lymphocyte activation and proliferative arteriopathies. *Am. J. Pathol.* 167:619–26.
18. Utans U, *et al.* (1996) Allograft inflammatory factory-1: a cytokine-responsive macrophage molecule expressed in transplanted human hearts. *Transplantation.* 61:1387–92.
19. Zhao YY, Yan DJ, Chen ZW. (2013) Role of AIF-1 in the regulation of inflammatory activation and diverse disease processes. *Cell. Immunol.* 284:75–83.
20. Schluesener HJ, Seid K, Kretzschmar J, Meyermann R. (1998) Allograft-inflammatory factor-1 in rat experimental autoimmune encephalomyelitis, neuritis, and uveitis: expression by activated macrophages and microglial cells. *Glia.* 24:244–51.
21. Lu J, *et al.* (2012) Pain in experimental autoimmune encephalitis: a comparative study between different mouse models. *J. Neuroinflammation.* 9:233.
22. Watano K, *et al.* (2001) Allograft inflammatory factor-1 augments production of interleukin-6, -10 and -12 by a mouse macrophage line. *Immunology.* 104:307–16.
23. Ohsawa K, Imai Y, Kanazawa H, Sasaki Y, Kohsaka S. (2000) Involvement of Iba1 in membrane ruffling and phagocytosis of macrophages/microglia. *J. Cell Sci.* 113:3073–84.
24. Casimiro I, Chinnasamy P, Sibinga NE. (2013) Genetic inactivation of the allograft inflammatory factor-1 locus. *Genesis.* 51:734–40.
25. Committee for the Update of the Guide for the Care and Use of Laboratory Animals, Institute for Laboratory Animal Research, Division on Earth and Life Studies, National Research Council of the National Academies. (2011) *Guide for the Care and Use of Laboratory Animals.* 8th edition. Washington (DC): National Academies Press.
26. Lutz SE, Raine CS, Brosnan CF. (2012) Loss of astrocyte connexins 43 and 30 does not significantly alter susceptibility or severity of acute experimental autoimmune encephalomyelitis in mice. *J. Neuroimmunol.* 245:8–14.
27. Pfaffl MW. (2001) A new mathematical model for relative quantification in real-time RT-PCR. *Nucleic Acids Res.* 29:e45.
28. Steinman L. (1999) Assessment of animal models for MS and demyelinating disease in the design of rational therapy. *Neuron.* 24:511–4.

29. Derecki NC, *et al.* (2012) Wild-type microglia arrest pathology in a mouse model of Rett syndrome. *Nature.* 484:105–9.
30. Furtado GC, *et al.* (2008) Swift entry of myelin-specific T lymphocytes into the central nervous system in spontaneous autoimmune encephalomyelitis. *J. Immunol.* 181:4648–55.
31. O'Connor RA, *et al.* (2008) Cutting edge: Th1 cells facilitate the entry of Th17 cells to the central nervous system during experimental autoimmune encephalomyelitis. *J. Immunol.* 181:3750–4.
32. Korn T, Mitsdoerffer M, Kuchroo VK. (2010) Immunological basis for the development of tissue inflammation and organ-specific autoimmunity in animal models of multiple sclerosis. *Results Probl. Cell Differ.* 51:43–74.
33. Cua DJ, *et al.* (2003) Interleukin-23 rather than interleukin-12 is the critical cytokine for autoimmune inflammation of the brain. *Nature.* 421:744–8.
34. Thakker P, *et al.* (2007) IL-23 is critical in the induction but not in the effector phase of experimental autoimmune encephalomyelitis. *J. Immunol.* 178:2589–98.
35. Sasaki Y, Ohsawa K, Kanazawa H, Kohsaka S, Imai Y. (2001) Iba1 is an actin-cross-linking protein in macrophages/microglia. *Biochem. Biophys. Res. Commun.* 286:292–7.
36. Imai Y, Kohsaka S. (2002) Intracellular signaling in M-CSF-induced microglia activation: role of Iba1. *Glia.* 40:164–74.
37. Autieri MV, Kelemen SE, Wendt KW. (2003) AIF-1 is an actin-polymerizing and Rac1-activating protein that promotes vascular smooth muscle cell migration. *Circ. Res.* 92:1107–14.
38. Heasman SJ, Ridley AJ. (2008) Mammalian Rho GTPases: new insights into their functions from in vivo studies. *Nat. Rev. Mol. Cell. Biol.* 9:690–701.
39. Yamada M, Ohsawa K, Imai Y, Kohsaka S, Kamitori S. (2006) X-ray structures of the microglia/macrophage-specific protein Iba1 from human and mouse demonstrate novel molecular conformation change induced by calcium binding. *J. Mol. Biol.* 364:449–57.
40. Schulze JO, *et al.* (2008) Structural and functional characterization of human Iba proteins. *FEBS J.* 275:4627–40.
41. Holsinger LJ, *et al.* (1998) Defects in actin-cap formation in Vav-deficient mice implicate an actin requirement for lymphocyte signal transduction. *Curr. Biol.* 8:563–72.
42. Becart S, *et al.* (2008) Tyrosine-phosphorylation-dependent translocation of the SLAT protein to the immunological synapse is required for NFAT transcription factor activation. *Immunity.* 29:704–19.
43. Kadoya M, *et al.* (2014) Allograft inflammatory factor-1 stimulates chemokine production and induces chemotaxis in human peripheral blood mononuclear cells. *Biochem. Biophys. Res. Comm.* 448:287–91.

Cite this article as: Chinnasamy P, *et al*. (2015) Loss of allograft inflammatory factor-1 ameliorates experimental autoimmune encephalomyelitis by limiting encephalitogenic CD4 T-cell expansion. *Mol. Med*. 21:233–41.